Eye-Lens Dose Reduction using Region of Interest (ROI) Attenuators in Neuroimaging

Martina P. Orji,[a*] Chao Guo,[b] Zhenyu Xiong,[c] S.V. Setlur Nagesh,[a] Stephen Rudin,[a] Daniel R. Bednarek[a]

[a] University at Buffalo, Canon Stroke and Vascular Research Center, Buffalo, NY, USA
[b] Cedars Sinai Medical Center, S. Mark Taper Foundation Imaging Center, Los Angeles, CA, USA
[c] Rutgers Cancer Institute of New Jersey, New Brunswick, NJ, USA

INTRODUCTION

- Cataracts and opacities could result following the exposure of the eye lens to radiation above a threshold dose.[1]
- The International Commission on Radiological Protection (ICRP) has determined a cataractogenesis threshold value to 0.5 Gy, a reduction below the previous threshold of 5 Gy.[2]
- In neuro-imaging procedures, primary focus is on the region of interest (ROI) containing the pathology, which requires detailed information needed for diagnosis and procedural guidance, whereas a lower-quality image could be acceptable in the periphery, which is primarily used for reference.[3-4]
- Use of an attenuator with a hole for the ROI as shown in Figure 1 reduces dose in the attenuated region, while allowing reference features to be seen.
- Equalization of the image brightness in the periphery to that in the ROI can be achieved by use of a Convolutional Neural Network (CNN),[5] which produces an ROI-boundary artifact-free, full-field image with equalized brightness and noise as seen in Figure 2.

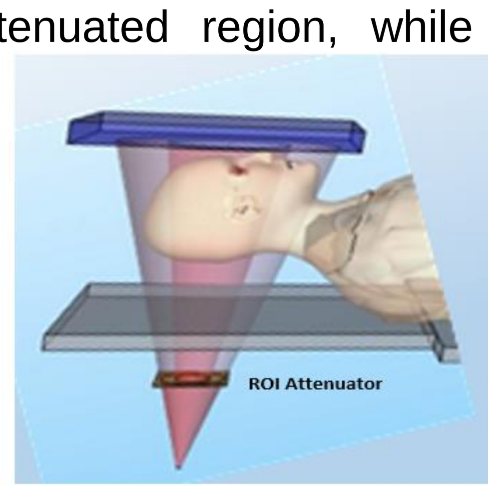

Figure.1 ROI imaging showing beam attenuator with round ROI aperture.

- This study estimated the dose reduction to the eye lens using ROI attenuators of varying transmission factor as a function of gantry angulation and head shift from isocenter.

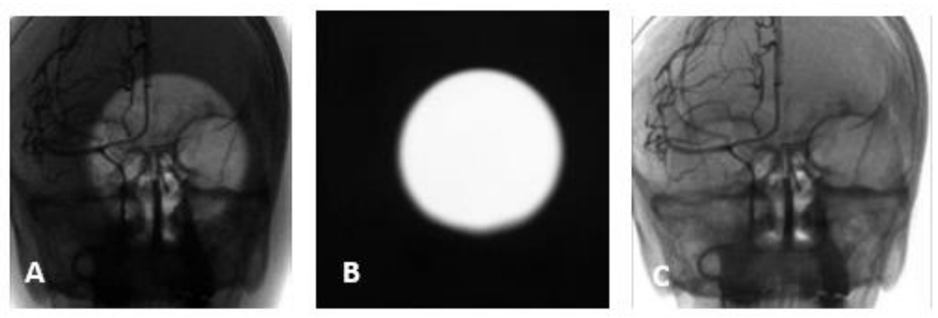

Figure 2. (A) Head image acquired with an ROI attenuator with a circular hole and 20% transmission factor showing the periphery with reduced intensity due to reduced dose. (B) Mask image of the ROI attenuator derived by CNN from Figure 2A. (C) Final brightness corrected, and noise reduced image obtained from Figure 2A using the mask of Figure 2B[5].

METHODS

- The eye lens dose was calculated for the Zubal computational phantom[6] using EGSnrc Monte-Carlo software as a function of gantry angulations from 0 to 90 degrees left anterior oblique (LAO) as shown in Figure 3, and for head shifts from isocenter as shown in Figure 4.
- The beam files were generated for 80 kVp beams with 1.8 mm aluminum added beam filtration and square field sizes of 5x5 cm (small FOV) and 10x10 cm (large FOV).[7]

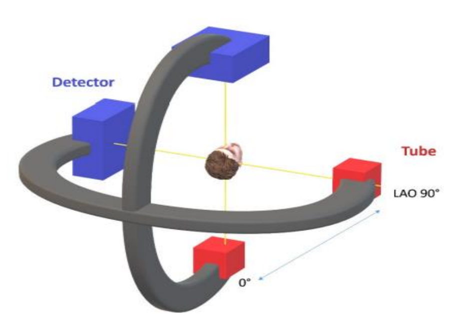

Figure 3: Gantry rotation angles from 0° to 90° LAO[7]

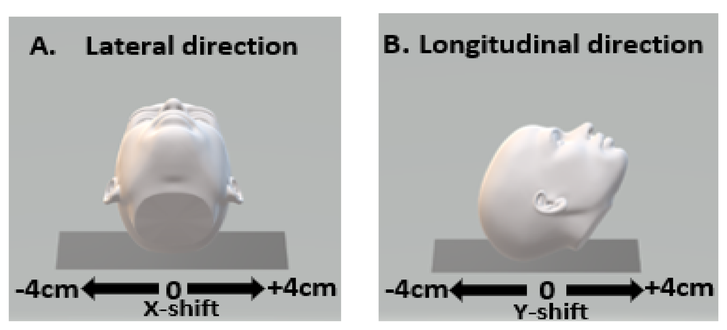

Figure 4. Shift of the center of the head relative to the beam isocenter as used for lens dose calculations: head shifts in (A) lateral X direction and (B) longitudinal Y direction.

- For this study, the ROI projection was simulated as the combination of the large square 10 x 10 cm FOV and the small square 5 x 5 cm FOV representing the ROI as shown in Fig. 5.
- The lens dose for a given projection with the ROI attenuator was then calculated as the weighted sum of the small-FOV lens dose (LD_S) and the large-FOV lens dose (LD_L).

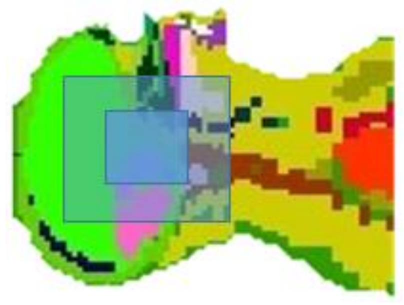

Figure 5: Lateral projection showing the combination of the small and large square FOV's to simulate the ROI attenuator exposure on the Zubal computational phantom.

- The dose to the eye lens per entrance air kerma with the ROI attenuator (LD_{ROI}) can be estimated as:

$LD_{ROI} = \{f \times LD_L + (1-f) \times LD_S\}$ .... (1)

where f, transmission factor, is the fraction of the beam exposure transmitted by the attenuator.

- The percent lens-dose reduction relative to the full field dose without attenuator is given as:

$\% \, LDR = 100 \times \{LD_L - LD_{ROI}\}/LD_L$ .... (2)

RESULTS

Note 1: The Zubal computational head is tilted such that the eyes are not symmetrically centered but shifted by about 1 cm to the right of the phantom centerline as seen in Fig. 6 where the lenses are depicted by red pixels on the head.

Note 2: The beam dimensions in Figures 6-10 are not to scale.

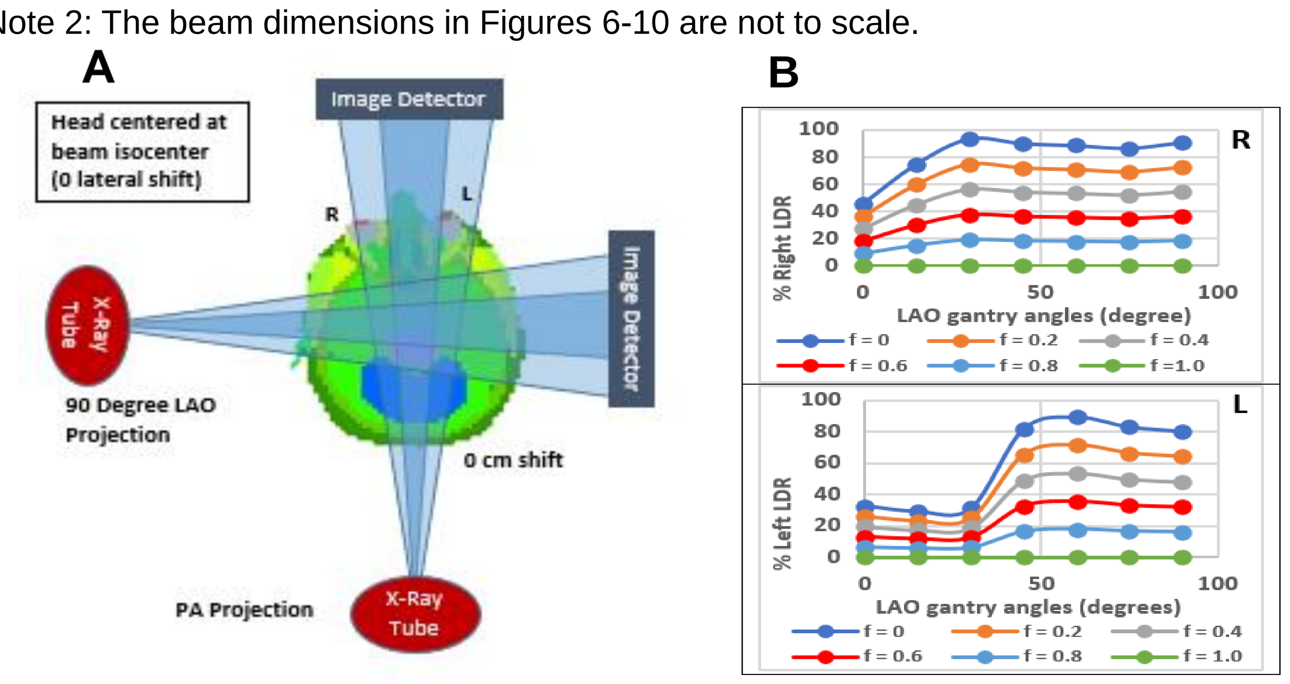

Figure 6: (A) Axial cross section showing head centered on the isocenter and the ROI attenuated beam for lateral and PA projections. (B) % LDR for right (R) and left (L) lenses as a function of LAO gantry angle for different transmission factors with 0cm head shift from isocenter.

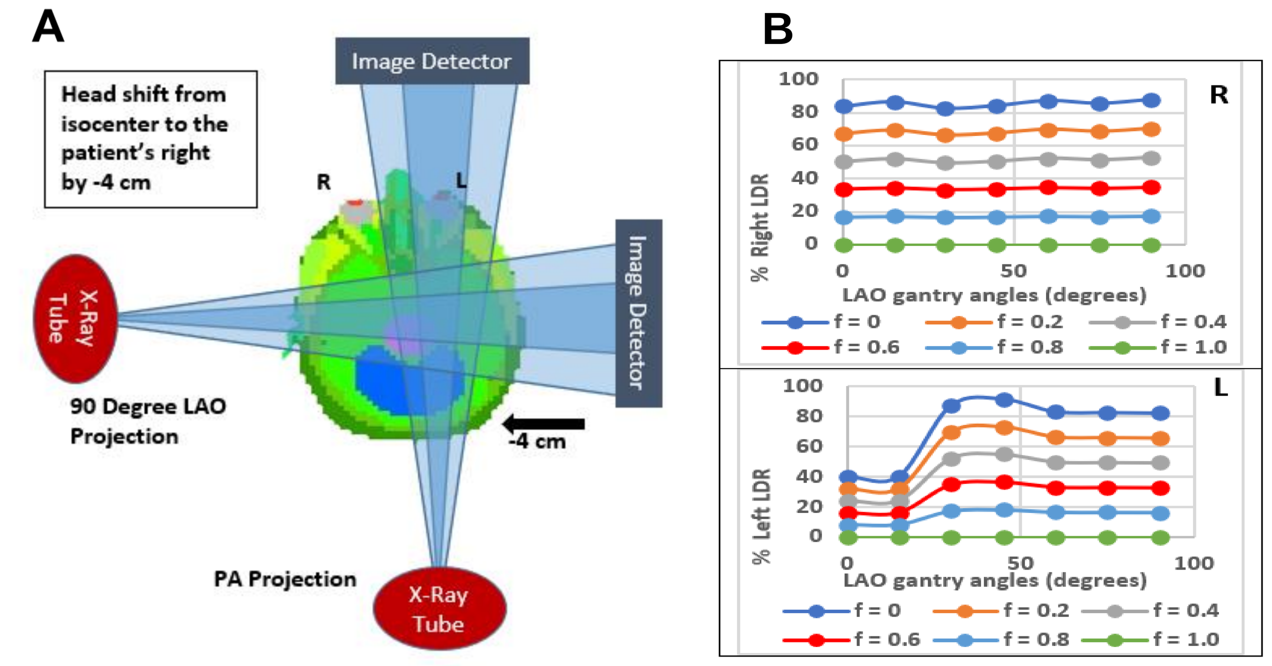

Figure 7: (A) Axial cross section showing head shift in the -x direction and ROI attenuated beam for lateral and PA projections. (B) % LDR for right (R) and left (L) lens as a function of LAO gantry angle for different transmission factors for a head shift from isocenter of -4 cm in the lateral direction.

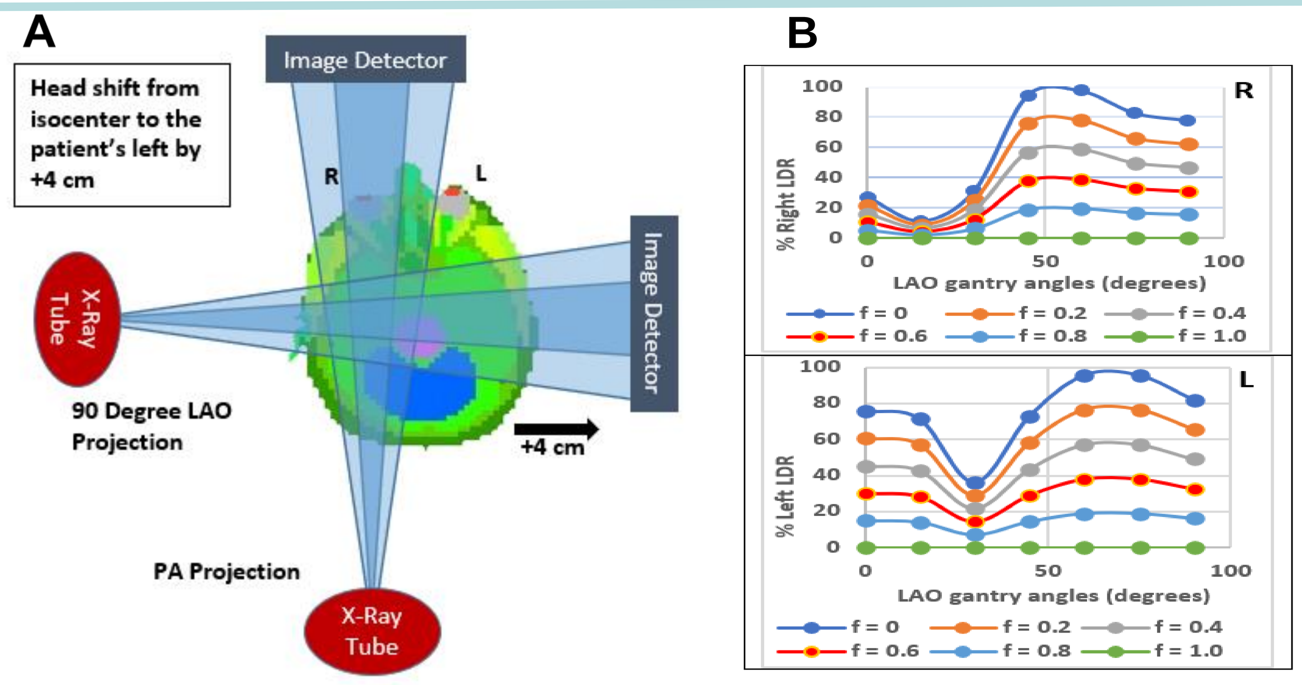

Figure 8: (A) Axial cross section showing head shift in the +x direction and ROI attenuated beam for lateral and PA projections. (B) % LDR for right (R) and left (L) lens as a function of LAO gantry angle for different transmission factors for a head shift from isocenter of +4 cm in the lateral direction.

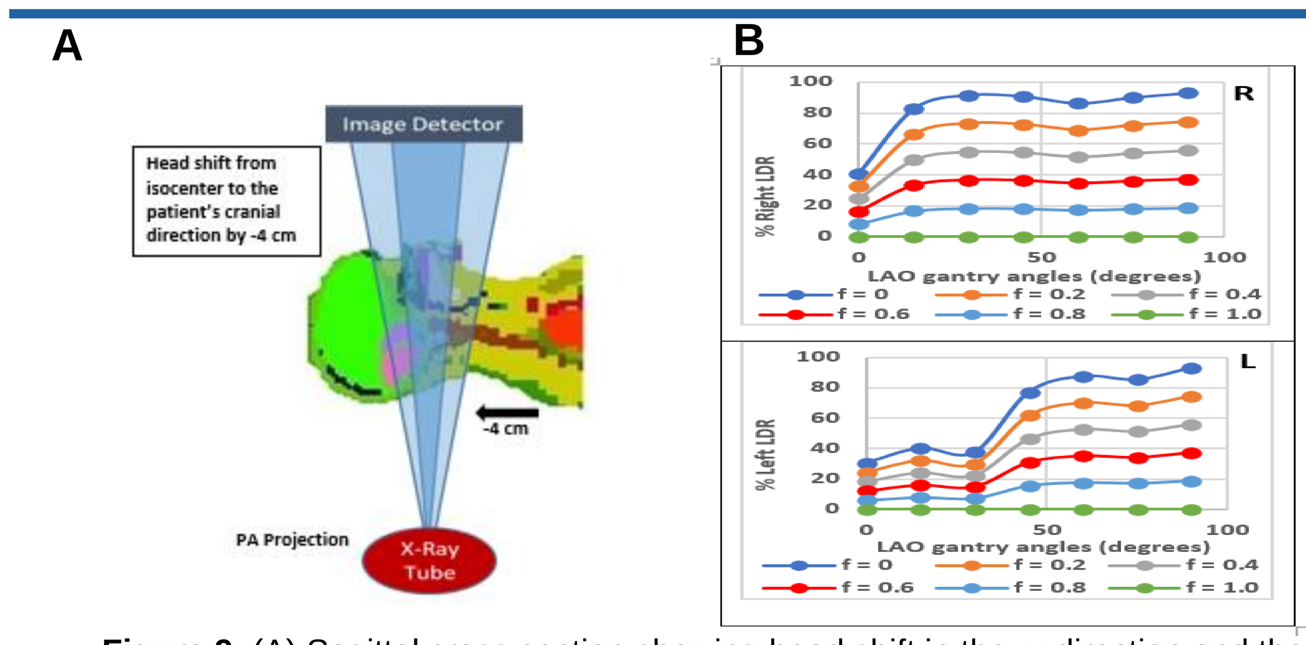

Figure 9: (A) Sagittal cross section showing head shift in the -y direction and the ROI attenuated beam for PA projection. (B) % LDR for right (R) and left (L) lens as a function of LAO gantry angle for different transmission factors (f) for a head shift from isocenter of -4 cm in the cranial direction.

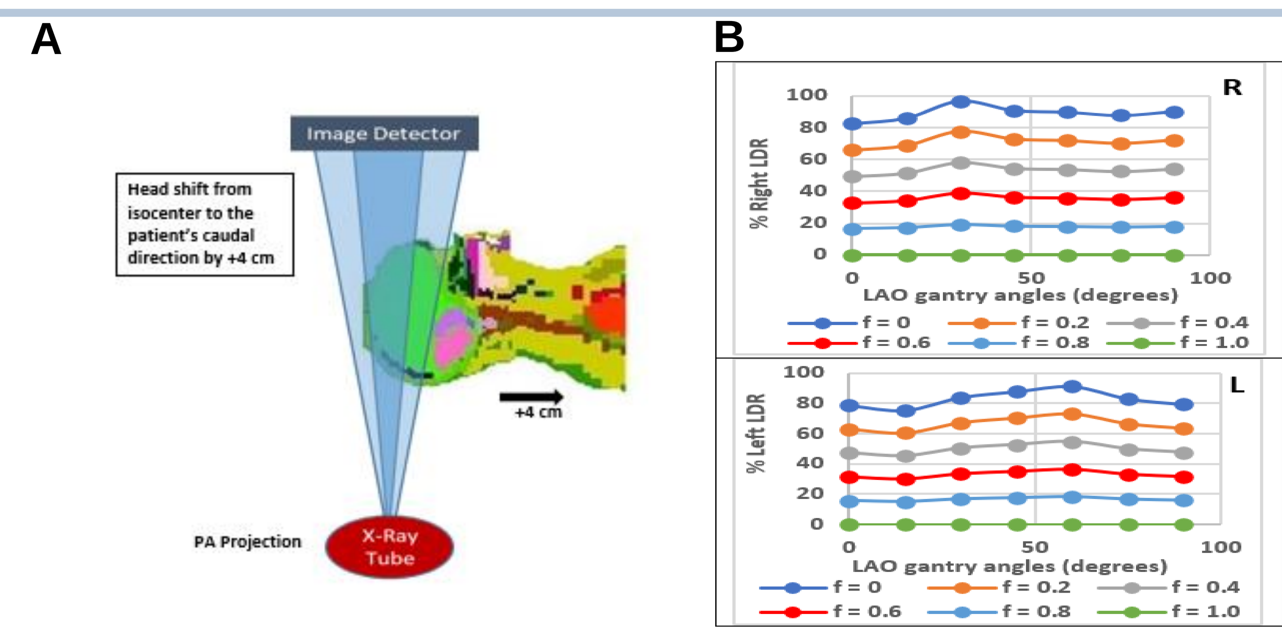

Figure 10: (A) Sagittal cross section showing head shift in the +y direction and ROI attenuated beam for PA projection. (B) % LDR for right (R) and left (L) lens as a function of LAO gantry angle for different transmission factors for a head shift from isocenter of +4 cm in the caudal direction.

DISCUSSION & CONCLUSIONS

- The lens dose reduction with the ROI attenuator is shown to vary with beam angulation and patient head position and between the left and right eyes.
- The least dose reduction occurs for angles when the eye lens is in the ROI, so the effect of the attenuator is on scatter dose.
- Due to about 1 cm lateral tilt of Zubal head phantom,[6] the right and left eyes are asymmetric relative to the head centerline, hence there is unequal dose reduction for the left and right lenses at 0 degrees LAO when the lateral shift is zero, as shown in Fig. 6.
- With a head shift of -4 cm and +4 cm in the x direction (lateral), the lens dose reduction varies with gantry LAO angle and, for a 20% transmission factor, increases up to about 75% at higher LAO angles compared to a 10 x 10 cm FOV for both lenses (Figs. 7 and 8).
- With a head shift of -4 cm and +4 cm along the y direction (longitudinal) there is a lens dose reduction of about 70% at LAO angles above 40 degrees for a 20% transmission factor with the ROI attenuator compared to a 10 x 10 cm FOV for both eye lens as shown in Figs. 9 and 10. Due to the lateral tilt of the Zubal head,[6] the % LDR is not the same for the left and right lenses even with a 0 cm lateral shift.
- The use of ROI attenuators allows visualization of full field information while providing a substantial reduction of lens dose, thereby reducing the risk of cataractogenesis during neuro-interventional procedures.

REFERENCES

1. Rehani MM, Vano E, Ciraj-Bjelac O, Kleiman NJ. Radiation and cataract. Radiat Prot Dosimetry 2011;147: 300–4.
2. International Commission on Radiological Protection, ICRP Statement on Tissue Reactions / Early and Late Effects of Radiation in Normal Tissues and Organs – Threshold Doses for Tissue Reactions in a Radiation Protection Context, ICRP Publication 118, Ann. ICRP 41 (1/2) (2012).
3. Rudin S, Bednarek DR. Region of interest fluoroscopy. Med Phys. 1992 Sep-Oct;19(5):1183-9. doi: 10.1118/1.596792.
4. Xiong Z, Vijayan S, Rudin S, Bednarek DR, "Assessment of organ and effective dose when using region-of-interest attenuators in cone-beam CT and interventional fluoroscopy," J. Med. Imag. 4(3), 031210 (2017), doi: 10.1117/1.JMI.4.3.031210.
5. S. V. Setlur Nagesh, A. Podgorsak, J. Krebs, D. R. Bednarek, S. Rudin, "Image processing using Convolutional Neural Network (CNN) for Region of Interest (ROI) fluoroscopy," Proc. SPIE 11317, Medical Imaging 2020: Biomedical Applications in Molecular, Structural, and Functional Imaging, 1131718 (28 February 2020); https://doi.org/10.1117/12.2549242
6. Zubal IG, Harrell CR, Smith EO, Rattner Z, Gindi GR, Hoffer PB, "Computerized Three-dimensional Segmented Human Anatomy," Med. Phys., 21 (2), 299 –302 (1994).
7. Guo C, Monte-Carlo Calculations for Patient and Staff Dose Management during Fluoroscopically Guided Procedures, PhD Dissertation, University at Buffalo, May 2020.

ACKNOWLEDGEMENT

The work was partially supported by Canon Medical Systems and NIH Grant No. 1R01EB030092 using the resources of the Center for Computational Research (CCR) of the University at Buffalo.

Corresponding Author email: mporji@buffalo.edu